A New Integral LQR based Primary Feedback Controller Design with Improved Power Quality for Multi-DGs based Microgrid Operation

1st Prakash Chandra Patra
Dept of Electrical & Electronics Engineering
GIET University
Gunupur, India
prakashchandra.patra@giet.edu

2nd Pratap Kumar Panigrahi
Dept of Electrical & Electronics Engineering
GIET University
Gunupur, India
pkpanigrahi@giet.edu

3rd Niranjan Nayak
Dept of Electrical & Electronics Engineering
SOA Deemed to be University
Bhubaneswar, India
niranjannayak@soa.ac.in

4th Snehamoy Dhar
Dept of Electrical & Electronics Engineering
SOA Deemed to be University
Bhubaneswar, India
snehamoydhar@gmail.com

***Abstract*— This paper presents a new Integral Linear Quadratic Regulator based Primary Feedback Controller (ILQR-PFC) for improving the power quality of a multi-distributed generation based microgrid. To improve the dynamic response and reduce steady-state tracking error, the conventional LQR formulation is augmented with integral current-error states. The proposed ILQR-PFC generates optimal (dq)-axis voltage control commands for the VSC by minimizing a quadratic cost function that balances current-tracking error and control effort. The performance of the proposed controller is validated in MATLAB/Simulink under renewable generation fluctuations and load-demand variations. Comparative results with conventional PID and standard LQR controllers show that the proposed ILQR-PFC provides improved DC-link voltage regulation, reduced battery discharge stress, faster oscillation damping, improved PCC frequency response, and reduced harmonic distortion. Therefore, the proposed controller offers a computationally simple and robust primary control solution for renewable energy based microgrid operation.**

Keywords*— Multi-DG microgrid, Integral LQR, primary feedback controller, voltage source converter, point of common coupling, battery backup, power quality, renewable energy

I. INTRODUCTION

The increasing penetration of renewable energy based distributed generation units has significantly changed the operational structure of modern microgrids. Photovoltaic and wind power generation systems are now widely integrated at the distribution level to reduce dependency on conventional generation and to support local energy demand [1]. However, the intermittent nature of solar irradiation and wind speed introduces frequent power imbalance, DC-link voltage fluctuation, and point of common coupling power-quality issues. These problems become more significant when multiple renewable distributed generation units are connected through power electronic converters to a common DC-link and then interfaced with an AC microgrid through a voltage source converter.

In a multi-DG renewable microgrid, the common DC-link acts as an intermediate power-balancing node. The photovoltaic systems inject power through DC–DC converters; the wind generation system contributes power through an AC–DC rectifier, and the battery backup unit exchanges power with the DC-link through a bidirectional DC–DC converter. During renewable power deficiency, the battery discharges to support the DC-link and the local load [2]. During excess renewable generation, the battery absorbs surplus power through charging operation. Therefore, the DC-side power management is strongly related to the stability of the DC-link voltage. On the AC side, the voltage source converter is responsible for transferring active power to the point of common coupling and for supporting reactive power compensation, frequency response, current quality, and harmonic reduction.

The point of common coupling is the most important location for evaluating power quality in the considered microgrid. Load variations, renewable generation fluctuations, converter switching, and grid interaction may produce oscillations in PCC current, frequency deviation, and harmonic distortion. Therefore, an effective primary feedback controller must regulate the VSC-side (dq)-axis current dynamics while maintaining a fast and robust response under changing operating conditions. Classical PID controllers are simple and easy to implement, but their performance may become limited under multi-variable coupling and uncertain renewable power variations. Advanced nonlinear controllers such as sliding mode control, (H_∞) control, and model predictive control[3] can improve performance, but they usually require higher computational effort and more complex implementation.

To overcome these limitations, this paper proposes an Integral Linear Quadratic Regulator based Primary Feedback Controller for the VSC of a multi-DG renewable microgrid. The VSC dynamics are represented in the (dq)-axis using PCC-based PLL information, where the (d)-axis current is associated with active power regulation and the (q)-axis current is associated with reactive power and PCC voltage support[4]. Unlike a standard LQR controller [5-6], the proposed scheme incorporates integral tracking-error states to reduce steady-state error and improve power-quality performance. The optimal feedback gain is obtained from the algebraic Riccati equation by minimizing a quadratic cost function containing both state-error penalty and control-effort penalty.

The main contributions of this paper are summarized as follows. First, a multi-DG renewable microgrid containing two PV systems, one wind power generation system, battery backup, common DC-link, VSC, utility grid, and local AC load is modeled for primary feedback control design[5]. Second, the VSC-side (dq)-axis current dynamics are considered as the principal control path for PCC power-quality improvement. Third, an ILQR-PFC is designed by augmenting the current tracking error with integral error states. Fourth, the proposed controller is compared with conventional PID and standard LQR controllers under simultaneous renewable generation and load-demand variations. The obtained results demonstrate improved oscillation damping, reduced DC-link fluctuation, better battery power utilization, and reduced harmonic distortion at the PCC.

XXX-X-XXXX-XXXX-X/XX/$XX.00 ©20XX IEEE

II. STUDIED MULTIPLE DGS BASED MICROGRID

The proposed new deterministic Primary Feedback Controller (PFC) is designed and tested on a multiple Renewable Energy based Distributed Generations (RE-DGs) environment, interconnected with Battery backup (Bbck) and local AC distribution system via Voltage Source Converter (VSC_{01}) as depicted in Fig. 1. Two numbers of Photovoltaic Systems (PVS: PVS_{01}, PVS_{02}), and one number of Wind Power generation System (WPS_{01}) are integrated with the common DC link, via individual unidirectional DC-DC Converters (i.e. DC-DC_1 and DC-DC_2), and unidirectional AC-DC Rectifier (AC-DC_1) respectively to get the multi-DGs environment. The Bbck system is incorporated with DC link via bidirectional DC-DC Converter (DC-DC_3) to balance the power demand at Point of Common Coupling (PCC) and provide reliable RE-DGs solution, under inconsistency at renewable energies. The PCC is integrated with this multi-DGs operation via VSC_{01} in a Phase Locked Loop (PLL) manner [5]. The PCC is connected to a small microgrid feeder including existing utility grid, and local AC load as in Fig. 1. The WPS_{01} is assumed with own gear-box control, and the AC-DC unidirectional converter is considered as uncontrolled (diode based) rectifier, towards ease of design complexity here, and will be included in future scope with rectifier control [10]. The detailed design parameters of the studied microgrid network are provided in Table 1.

The Local Power Management (LPM) decision is estimated at DC link and PCC, where terminal voltage ($\boldsymbol{V}_{DC}$) and output powers of individual DC-DC Converters (i.e. DC-DC_{01}, DC-DC_{02}, and DC-DC_{03}), AC-DC Rectifier's (AC-DC_{01}), and VSC_{01} to PCC relations are considered for DC link, and PCC side LPMs respectively. The DC side LMP system decision is obtained as:

$$\pm P_{DC} = \pm\eta_{batt} P_{batt} + \left(\sum_{i=1}^{2} P_{PV,i} + P_{WPS} \right) \quad (1)$$

where, $\boldsymbol{P}_{DC}$ = VSC input/ output power (depending on Load demand, RES generations), $\pm\,\boldsymbol{P}_{batt}$ = battery power in (– for charging) or out (+ for discharging), $\boldsymbol{\eta}_{batt}$ = battery charging/ discharging indicators from Tertiary Controller (TC) level decisions.

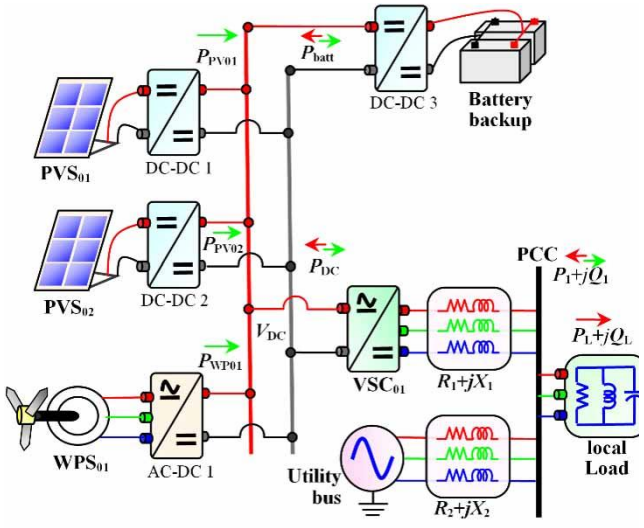

Figure 1. Schematic of Studied multiple Distributed Generations (DGs: 2 nos. PVs, and 1 no. WPS) based Microgrid operation with Battery backup

Photovoltaic based RE-DGs	
PV panel (individual) at Standard test conditions/STC	$\boldsymbol{P}_{MP}$: 1.1 kW, $\boldsymbol{V}_{OC}$: 19.7 V, $\boldsymbol{I}_{SC}$: 55.8 A, NOTC: (45 ± 3) ºC
PV DC-DC Converters (rated)	2×1.4 kW (each): 2.8 kW, $\boldsymbol{V}_{MP}$: 16.8 V at STC as input, and output at $\boldsymbol{V}_{DC}$: 24 V
Wind Power generation System based RE-DG	
Wind Turbine Generator (individual) at STC	$\boldsymbol{P}_{WP}$: 1.5 kW, $\boldsymbol{V}_{WP}$: 38 V at 12 m/sec. speed (with cut-in/ cut-out: 3-25 m/sec.)
WPS AC-DC Rectifier (rated)	1×1.8 kW, $\boldsymbol{I}_S$: 75 A, at $\boldsymbol{V}_{DC}$: 24 V
VSC and Local Loads	
Three Phase VSC (rated)	$\boldsymbol{S}_{VSC01}$: 5 kVA for input $\boldsymbol{V}_{DC}$: 24 V, output $\boldsymbol{V}_{LL}$: 415V at 50 Hz
Overhead AC conductors (AAC) and Local AC Loads	$\boldsymbol{L}_1$: 4.8 mH/kms, $\boldsymbol{R}_1$: 0.047 Ω/kms; 1–5 kW + 140 kVAR at 50 Hz

The $\boldsymbol{P}_{PV}$ = PV power at subjected test conditions, and $\boldsymbol{P}_{WPS}$ = Wind power at given wind speed. The PCC side LMP is designed as:

$$\pm P_{VSC} + j\,Q_{VSC} = \frac{3}{2}\left[\begin{pmatrix} V_{d,PCC} \times I_{d,VSC01} \\ +V_{q,PCC} \times I_{q,VSC01} \end{pmatrix} + j \begin{pmatrix} V_{q,PCC} \times I_{d,VSC01} \\ -V_{d,PCC} \times I_{q,VSC01} \end{pmatrix} \right] \quad (2)$$

where, $\boldsymbol{P}_{VSC} + j\boldsymbol{Q}_{VSC}$ = is VSC output AC power, $\boldsymbol{V}_{d,PCC} + j\,\boldsymbol{V}_{q,PCC}$= measured PCC side *abc-dq* axis represented voltage, and $\boldsymbol{I}_{d,VSC01} + j\,\boldsymbol{I}_{q,VSC01}$ = measured PCC side *abc-dq* axis represented voltage, and current parameters respectively.

The PV side DC-DC converters are considered to be Voltage Boost (VBo) operational and the Bbck system is designed to be operated VBo, Voltage Buck (VBu) models depending on discharging/ charging decisions[4]. These converters are considered with well-designed MPPT based PFCs for duty cycle based switching operations. To design a PFC based closed-loop system to improved power-quality at PCC the VSC_{01} is the targeted converter here. The VSC's AC side *abc-dq* axis represented voltage (control input parameter) and current (state output parameters), along with PCC measured voltage parameters are considered for VSC's dynamic relations as:

$$\frac{d}{dt}\begin{bmatrix} I_{d,VSC01} \\ I_{q,VSC01} \end{bmatrix} = \begin{bmatrix} -\frac{R_1}{L_1} & \omega_{PLL} \\ -\omega_{PLL} & -\frac{R_1}{L_1} \end{bmatrix} \times \begin{bmatrix} I_{d,VSC01} \\ I_{q,VSC01} \end{bmatrix} + \frac{1}{L_1}\begin{bmatrix} V_{d,VSC01} \\ V_{q,VSC01} \end{bmatrix} - \frac{1}{L_1}\begin{bmatrix} V_{d,PCC} \\ V_{q,PCC} \end{bmatrix} \quad (3)$$

$$\dot{x} = [\mathbf{A}]x + [\mathbf{B}]u + [\mathbf{E}]d$$

where, $\boldsymbol{V}_{d,VSC01} + j\,\boldsymbol{V}_{q,VSC01}$ = VSC AC side *abc-dq* axis represented voltage, $\boldsymbol{R}_1 + j\boldsymbol{\omega}_{PLL}\boldsymbol{L}_1$ = AC overhead line impedance. The Load demand at PCC is compensated by VSC, indirectly via DC link RE-DGs LMP operation to keep the $\boldsymbol{P}_{DC}$ level up to the requirements. The state-space represented equations are standard $\boldsymbol{x}$ = state parameters, $\boldsymbol{u}$ = control inputs, $\boldsymbol{d}$ = measured disturbances, along with their respective transformation mappings: $\mathbf{A}$ = state-matrix, $\mathbf{B}$ = control-matrix, $\mathbf{E}$ = disturbance-matrix.

The PFC is targeted to be fast acting (> 30 kHz sampling rates) for possible future industrial up-gradation, where silent

operation along with fast transient response will be expected. The Power Quality (PQ) challenges like low-frequency harmonics are targeted to be reduced by proposing such operation, along with high electromagnetic interference. To operate a PFC at fast switching, here the execution is targeted to be less computational (hardware interpretable), yet robust in terms of performance.

III. PROPOSED NEW ILQR BASED PRIMARY FEEDBACK

Majority of feedback paths are designed with simple linear Proportional-Integral-Derivative (PID) controllers, which poses performance hazards (under-fitted) under high uncertainty volatility. Few PFCs are designed[7] with computational, non-linear feedbacks: sliding mode control (SMC), H-infinity, Model Predictive Control (MPC) for better accuracy. But the design complexity and implementation cost for such non-linear algorithms are limiting its application. Here a dynamic yet robust feedback path is considered in terms of a new Integral Linear Quadratic Regulator (ILQR) scheme. The LQR is well known for its robust performance[8-9], but its tracking become limited under multi-parametric state variations (e.g. three-phase VSC feedback). An integral state of tracking error is further incorporated here for improved performance.

The Feedback path tracking error is estimated as:

$$e_x = \begin{bmatrix} e_{\mathrm{d}} \\ e_{\mathrm{q}} \end{bmatrix} = \begin{bmatrix} I^{*}_{\mathrm{d,VSC01}} - I_{\mathrm{d,VSC01}} \\ I^{*}_{\mathrm{q,VSC01}} - I_{\mathrm{q,VSC01}} \end{bmatrix} \quad (4)$$

Here, the current d-q axis references are estimated from TC decisions. To improve the steady-state performance for better Power Quality at PCC the Integral error is derived as:

$$z_x = \begin{bmatrix} z_{\mathrm{d}} \\ z_{\mathrm{q}} \end{bmatrix} = \begin{bmatrix} \int e_{\mathrm{d}} dt \\ \int e_{\mathrm{q}} dt \end{bmatrix}$$

or

$$\dot{z}_x = \begin{bmatrix} \dot{z}_{\mathrm{d}} \\ \dot{z}_{\mathrm{q}} \end{bmatrix} = \begin{bmatrix} I^{*}_{\mathrm{d,VSC01}} - I_{\mathrm{d,VSC01}} \\ I^{*}_{\mathrm{q,VSC01}} - I_{\mathrm{q,VSC01}} \end{bmatrix} \quad (5)$$

The augmented state error for proposed ILQR-PFC is defined as:

$$e_{\mathrm{ILQR}} = \begin{bmatrix} e_{\mathrm{d}} \\ e_{\mathrm{q}} \\ z_{\mathrm{d}} \\ z_{\mathrm{q}} \end{bmatrix} = \begin{bmatrix} I^{*}_{\mathrm{d,VSC01}} - I_{\mathrm{d,VSC01}} \\ I^{*}_{\mathrm{q,VSC01}} - I_{\mathrm{q,VSC01}} \\ \int \left(I^{*}_{\mathrm{d,VSC01}} - I_{\mathrm{d,VSC01}} \right) dt \\ \int \left(I^{*}_{\mathrm{q,VSC01}} - I_{\mathrm{q,VSC01}} \right) dt \end{bmatrix} \quad (6)$$

The control input dynamics ($\Delta \boldsymbol{u}$) are derived from proposed ILQR-PFC as:

$$\Delta u = \begin{bmatrix} \Delta V_{\mathrm{d,\,VSC01}} \\ \Delta V_{\mathrm{q,\,VSC01}} \end{bmatrix} = -K_{\mathrm{ILQR}} \times e_{\mathrm{ILQR}}$$

where

$$K_{\mathrm{ILQR}} = \begin{bmatrix} K_{P,\mathrm{d}} & 0 & K_{Z,\mathrm{d}} & 0 \\ 0 & K_{P,\mathrm{q}} & 0 & K_{Z,\mathrm{q}} \end{bmatrix} \quad (7)$$

Here $\boldsymbol{K}_{\mathrm{ILQR}}$ = ILQR-PFC path gains, incorporating $\boldsymbol{K}_{\mathrm{Pd}}$ and $\boldsymbol{K}_{\mathrm{Pq}}$= proportional gains; $\boldsymbol{K}_{\mathrm{Zd}}$ and $\boldsymbol{K}_{\mathrm{Zq}}$= integral gains, respectively. To find the optimal gains for feedback path the Algebraic Riccati (AR) solution is obtained by minimizing quadratic cost function (J_{PFC}) as:

$$K_{\mathrm{ILQR}} = \mathbf{R}^{-1}_{\mathrm{ILQR}} \mathbf{B}^{T}_{\mathrm{Z}} \mathbf{P}_{\mathrm{ILQR}}$$

while

$$\min \left| J_{\mathrm{PFC}} \right| = \int_{0}^{\infty} \left(\boldsymbol{x}^{T} \mathbf{Q}_{\mathrm{ILQR}} \boldsymbol{x} + \boldsymbol{u}^{T} \mathbf{R}_{\mathrm{ILQR}} \boldsymbol{u} \right) \quad (8)$$

Here $\mathbf{R}_{\mathbf{ILQR}}$ =Regulation cost matrix, $\mathbf{P}_{\mathbf{ILQR}}$ = Primary solution matrix, $\mathrm{Q}_{\mathbf{ILQR}}$ = State cost matrix for standard LQR optimality formulation. The $\boldsymbol{x}^{T}\,\mathrm{Q}_{\mathbf{ILQR}}\boldsymbol{x}$= state error penalty, $\boldsymbol{u}^{T}\,\mathrm{R}_{\mathbf{ILQR}}\boldsymbol{u}$ = control effort penalty are balanced while minimizing the cost function. While considering Lyapunov stability the $\mathbf{P}_{\mathbf{ILQR}}$ is obtained from:

$$\dot{V}_{\mathrm{PFC}} = -\boldsymbol{x}^{T} \left(\mathbf{Q}_{\mathrm{ILQR}} + K^{T}_{\mathrm{ILQR}} \mathbf{R}_{\mathrm{ILQR}} K_{\mathrm{ILQR}} \right) \boldsymbol{x} \; < 0 \quad (9)$$

Here the Lyapunov function is considered as $\boldsymbol{V}_{\mathrm{PFC}} = \boldsymbol{x}^{T}\,\mathrm{Q}_{\mathbf{ILQR}}\boldsymbol{x}$. The performance of the proposed ILQR-PFC based VSC to PCC dynamics is presented in section 4.

IV. RESULT ANALYSIS

The performance of the proposed ILQR-PFC based VSC Feedback is elaborated in terms of detailed mathematical modeling with switching considerations, in MATLAB Simulink® platform. The detailed mathematical model based switching model is obtained as in Fig. 1. The sampling frequency is kept around 33 kHz for present study. The comparisons of proposed ILQR-PFC (here Prop_{0}) is made with standard PID controller (here Conv_{02}), and LQR controller (here Conv_{01}). The efficacy is measured while subjecting PV Solar Irradiation (W/m^2) variations, with simultaneous Load demand changes ($\boldsymbol{P}_{\mathrm{Load}} = \boldsymbol{P}_{\mathrm{PCC}}$). The performance of proposed PFC is established in terms of steady state oscillation damping, presence of harmonics in measured PCC profiles.

The increased switching frequency operation (>30 kHz) provides faster, more frequent voltage transitions ($\mathrm{d}\boldsymbol{V}_{\mathrm{DC}}/\mathrm{d}t$) generate stronger high-frequency electromagnetic interference (EMI), influence into the DC link performance. The low-frequency harmonics are minimized both sides of VSC operation due to such switching. The switching at 33 kHz around provides faster, more frequent voltage transitions ($\mathrm{d}\boldsymbol{V}_{\mathrm{DC}}/\mathrm{d}t$), which generate stronger high-frequency electromagnetic interference (EMI), radiate back to DC link performance too. The performance improvements are significantly visible at both: DC link and PCC sides of the studied VSC_{01}.

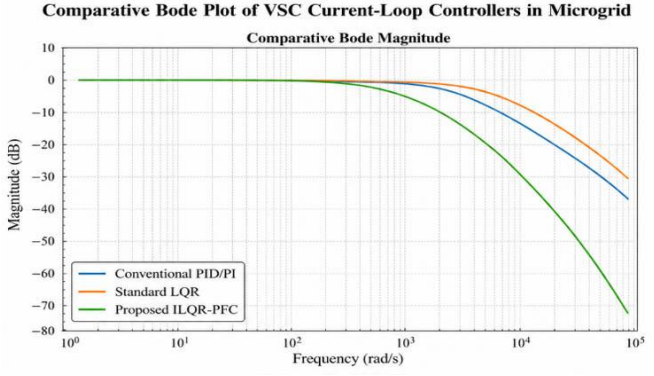

(a)

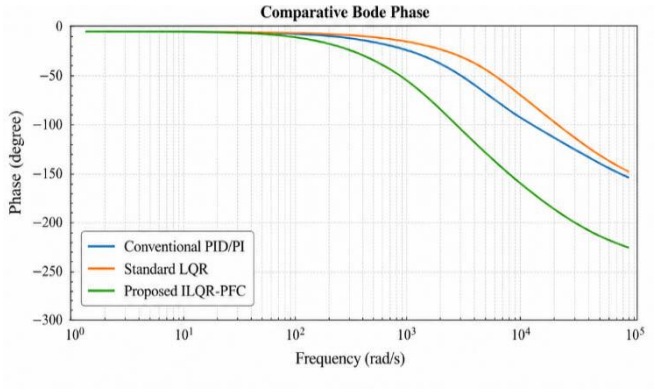

(b)

Figure 2. Stability of proposed ILQR-PFC, compared with conventional PFCs: (a) Magnitude, and (b) Phase margin.

The comparative Bode response provides a small-signal frequency-domain justification for the improved dynamic behavior of the proposed ILQR-PFC in the VSC current-control loop. At low frequency, all three controllers maintain approximately unity gain, which indicates that the dq-axis current references can be tracked properly during steady-state operation. However, the difference becomes visible in the mid- and high-frequency regions (Fig. 2.a). The conventional PID/PI controller shows a slower roll-off, which means that high-frequency disturbances, switching ripple, and converter-side perturbations may pass more easily into the controlled current response. The standard LQR improves the dynamic shaping because its gain is obtained through an optimal state-feedback formulation, but it does not include integral current-error compensation. In contrast, the proposed ILQR-PFC shows stronger attenuation (Fig. 2.b) in the higher-frequency region, indicating better rejection of unwanted oscillatory components and converter-induced disturbances. This supports the manuscript observation that the ILQR-PFC reduces PCC-side oscillations and harmonic distortion more effectively than the conventional PID and standard LQR controllers.

Further the proposed ILQR provides a new Integral path error tracking, minimizing the steady state error significantly (Figs. 3-6). The PVS_{01}, PVS_{02} are subjected to solar irradiation variations, at every 10 sec. intervals and the DC link voltage and individual DGs power outputs ($\boldsymbol{P}_{PV01}$, $\boldsymbol{P}_{PV02}$ respectively) are recorded as in Fig. 3.

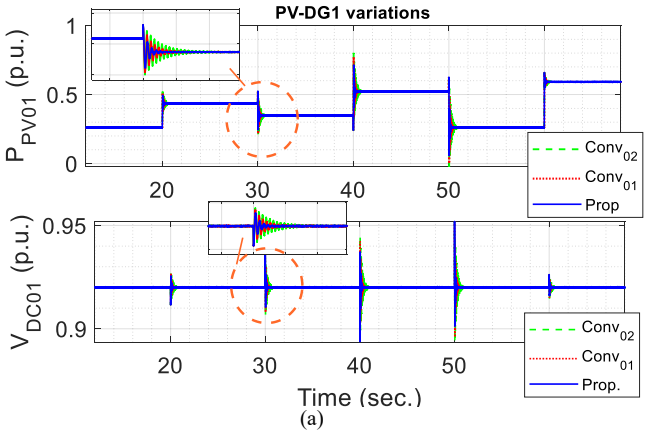

(a)

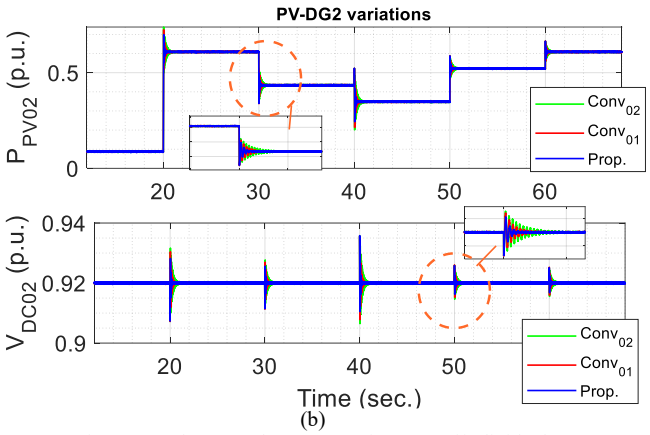

(b)

Figure 3. Performance of proposed ILQR-PFC in terms of individual PV-DGs power profiles and DC link voltage profiles for: (a) PV system 01, and (b) PV system 02.

The proposed ILQR-PFC provides improved dynamic oscillation damping (almost 56 – 62 cycles), as compared with conventional PID (>175 cycles), and LQR (78 – 92 cycles) controllers.

The subjected dynamic PV changes and DC side LPM operation for Battery backup operation (Eq. 1) is validated under simultaneous PV (10 sec. regular intervals), and load demand (15 sec. regular intervals) as in Fig. 4(a). The scarcities of RES based DG generations are compensated by the Bbck system as in this figure. The State-of-Charge (SoC in %) is depicted in Fig. 4(b), under such operational variations. The proposed ILQR-PFC provides improved SoC dischaging (almost 2-4% discharge level), as compared with conventional PID (>10 % discharge level), and LQR (4-6% discharge level) controllers.

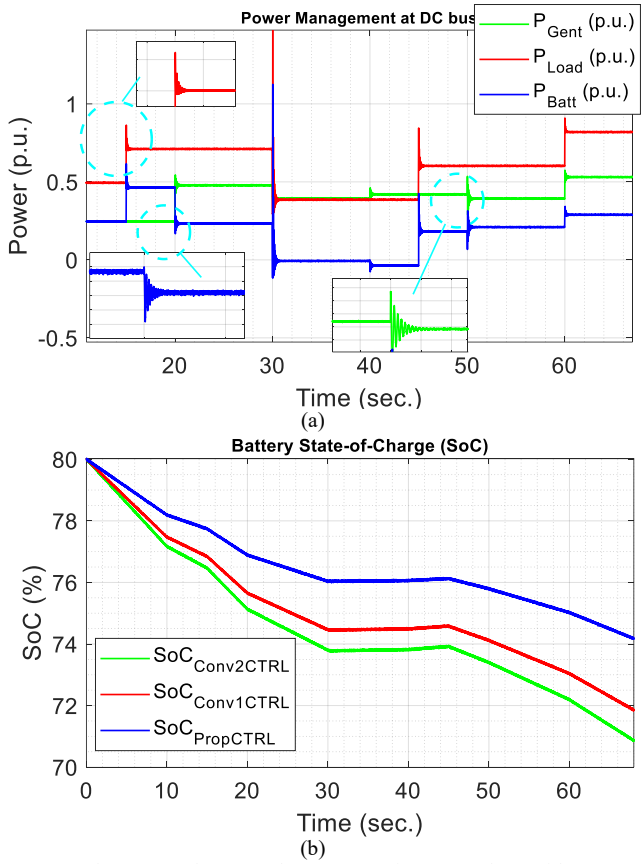

(a) (b)

Figure 4. Performance of proposed ILQR-PFC in terms of DC side LPM operation: (a) total Power Generation, load demand at PCC, and Battery

power profiles, and (b) State-of-Charge (SoC in %) variations for different controllers.

The Total Harmonic Distortions (THD in %) is recorded as in Fig. 5(b), where the proposed ILQR-PFC is recorded with improved THD reduction (> 5 %), as compared with conventional PID (15-20%), and LQR (4-11%) controllers. The PCC side frequency is estimated from voltage and current profiles and the frequency variation under PV and Load demand changes is presented in Fig. 4. Here both 10 sec. and 15 sec. intervals are overlapped against PV and Load variations as in Fig. 5(a). The proposed ILQR-PFC is recorded with reduced low-frequency oscillation damping, and PQ improved frequency response (35-48 cycles), as compared with conventional PID (98-110 cycles), and LQR (56-74 cycles) controllers.

Further the performance of the proposed PFC is established in terms of load variations recorded at PCC side three-phase currents, as in Fig. 6. The proposed ILQR-PFC feedback is depicted with 35-56 cycles of dynamic oscillations, and with improved PQ performance as in Fig. 6(a).

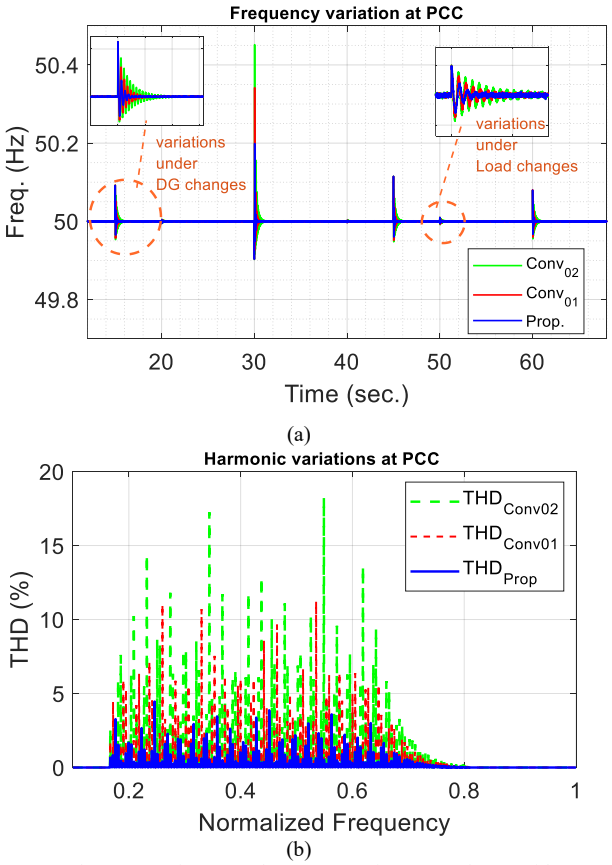

Figure 5. Performance of proposed ILQR-PFC in terms of PCC side LPM operation: (a) Frequency (Hz) response at PCC, and (b) Total Harmonic distortion (THD in %) variations for different controllers.

The conventional LQR based PFC is depicted with 48-78 cycles of oscillations and increased PQ profiles, as in Fig. 6(b). The conventional PID controller id recorded with 64-98 cycles of dynamic oscillations; with sever harmonic profile, as in Fig. 6(c).

Further a real-time validation study is evidenced for proposed ILQR-PFC, in terms of controller execution, RTI interfaced with dSPACE 1104. The multi-DGs based microgrid architecture (Fig. 1) is targeted here to be implemented as ControlDesk® based RTI simulation, and the ILQR-PFC feedback is designed in dSPACE1104's master processor. The PCC responses are recorded from Hardware-in-Loop (HiL) manner at SEGLEN Digital Storage Oscilloscope (DSO), as in Fig. 7. The phase-A Voltage: $\boldsymbol{V}_{PCC,a}$ (Fig. 15.a), and active power: $\boldsymbol{P}_{PCC}$ (in Fig. 7.b) are plotted and evidenced the similar performance superiority over conventional PFCs.

The proposed ILQR-PFC is evidenced significantly improving the PCC profiles, with damping dynamic oscillations as well as reducing harmonic profiles, as compared with classical PID and LQR based feedback paths. The proposed controller is going to be studied for Hardware-in-Loop (HiL) based test-bench operation [11] as immediate future scope of this paper.

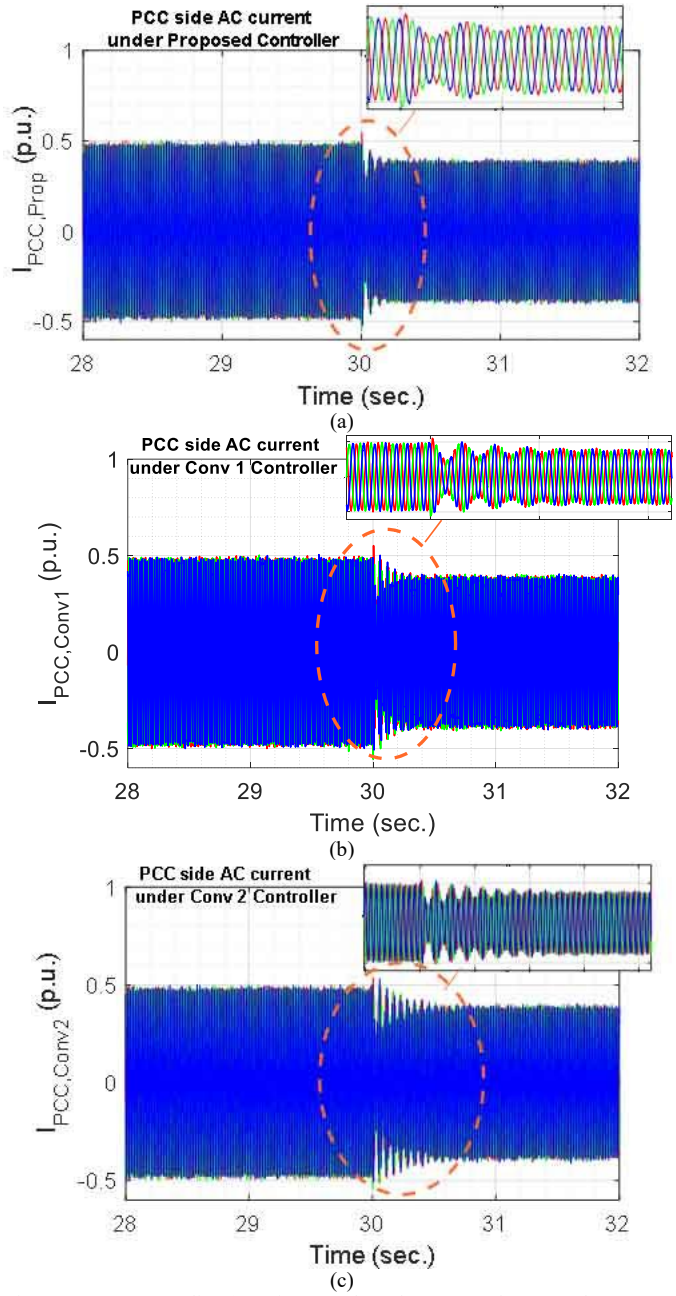

Figure 6. Power Quality (PQ) improved Performance of proposed ILQR-PFC in terms of PCC side 3-ph AC current from: (a) Conv.$_{-02}$, (b) Conv.$_{-01}$, and (c) Prop. ILQR-PFC responses, under Local AC load variations.

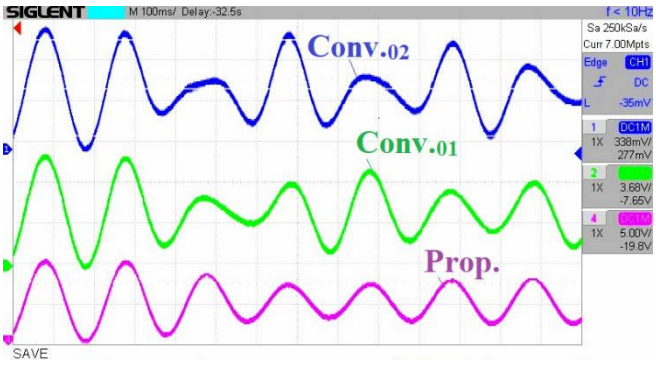

(a)

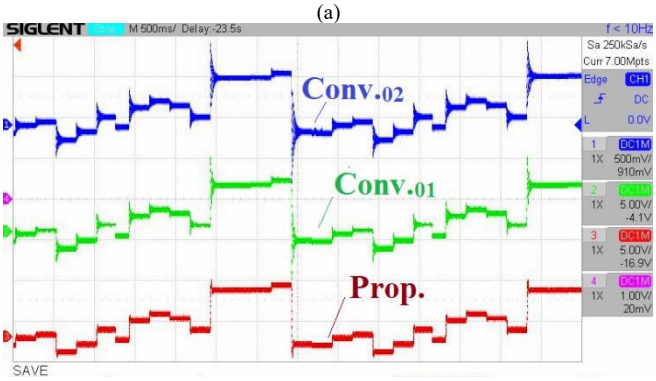

(b)

Figure 7. dSPACE RTI based Hardware validation of proposed ILQR-PFC in terms of PCC side power changes for: (a) Conv.$_{02}$, (b) Conv.$_{01}$, and (c) Prop. ILQR-PFC responses, under Local AC load variations

V. CONCLUSION

This paper presented an Integral Linear Quadratic Regulator based Primary Feedback Controller for improving the dynamic and power-quality performance of a multi-DG renewable energy based microgrid. The studied system included two photovoltaic systems, one wind power generation system, a battery backup unit, a common DC-link, and a voltage source converter connected to the point of common coupling. The renewable DG units and battery backup were coordinated through the DC-link power management structure, while the VSC was considered as the main controllable interface for PCC-side power-quality improvement.

The VSC dynamics were modeled in the synchronous (dq)-reference frame using PCC-based PLL information. Since the (d)-axis current directly influences active power transfer and the (q)-axis current influences reactive power and PCC voltage support, the proposed feedback controller was designed around the (dq)-axis current dynamics. To overcome the steady-state tracking limitation of conventional LQR control, integral current-error states were incorporated into the feedback model. The resulting ILQR-PFC produced optimal voltage control commands for the VSC by minimizing a quadratic cost function that simultaneously penalized tracking error and control effort.

The MATLAB/Simulink and dSPACE RTI based results verified that the proposed ILQR-PFC provides better performance than conventional PID and standard LQR controllers. Under solar irradiation changes and load-demand variations, the proposed controller achieved improved DC-link voltage regulation, reduced dynamic oscillations, better battery power utilization, lower SoC discharge stress, improved PCC frequency response, and reduced harmonic distortion. The PCC current profiles also showed improved damping and reduced distortion under the proposed controller. Therefore, the proposed ILQR-PFC can be considered a fast, robust, and computationally suitable primary control strategy for renewable energy based microgrid operation.

REFERENCES

[1] Arfeen, Zeeshan Ahmad, Azhar B. Khairuddin, Raja Masood Larik, and Mohammad Salman Saeed. "Control of distributed generation systems for microgrid applications: A technological review." *International Transactions on Electrical Energy Systems* 29, no. 9 (2019): e12072.

[2] Saleh, Abdolhossein, Ali Deihimi, and Reza Iravani. "Model predictive control of distributed generations with feed-forward output currents." *IEEE Transactions on Smart Grid* 10, no. 2 (2017): 1488-1500.

[3] Bouzid, Allal M., Josep M. Guerrero, Ahmed Cheriti, Mohamed Bouhamida, Pierre Sicard, and Mustapha Benghanem. "A survey on control of electric power distributed generation systems for microgrid applications." *Renewable and Sustainable Energy Reviews* 44 (2015): 751-766.

[4] Satpathy, Anshuman, Snehamoy Dhar, P. K. Dash, Ranjeeta Bisoi, and Niranjan Nayak. "A new representation learning based maximum power operation towards improved energy management integration with DG controllers for photovoltaic generators using online deep exponentially expanded RVFLN algorithm." *Applied Soft Computing* 166 (2024): 112185.

[5] Priyadarshini, Lipsa, P. K. Dash, and Snehamoy Dhar. "A new exponentially expanded robust random vector functional link network based MPPT model for local energy management of PV-battery energy storage integrated microgrid." *Engineering Applications of Artificial Intelligence* 91 (2020): 103633.

[6] Sen, Sachidananda, and Vishal Kumar. "Decentralized output-feedback-based robust LQR Vf controller for PV-battery microgrid including generation uncertainties." *IEEE Systems Journal* 14, no. 3 (2020): 4418-4429.

[7] Valencia-Rivera, Gerardo Humberto, Luis Ramon Merchan-Villalba, Guillermo Tapia-Tinoco, Jose Merced Lozano-Garcia, Mario Alberto Ibarra-Manzano, and Juan Gabriel Avina-Cervantes. "Hybrid LQR-PI control for microgrids under unbalanced linear and nonlinear loads." *Mathematics* 8, no. 7 (2020): 1096.

[8] Sen, Sachidananda, and Vishal Kumar. "Robust decentralized output-feedback type LQR voltage controller for inverter-based microgrid." In *2019 10th International Conference on Computing, Communication and Networking Technologies (ICCCNT)*, pp. 1-6. IEEE, 2019.

[9] Kumar, Rohit Ranjan, Anil Kumar Yadav, and Maloth Ramesh. "Hybrid PID plus LQR based frequency regulation approach for the renewable sources based standalone microgrid." *International Journal of Information Technology* 14, no. 5 (2022): 2567-2574.

[10] Kumar, Raushan, and Sheetla Prasad. "Optimal Frequency Regulation Scheme in a Wind Power Integrated AC Microgrid." *IEEE Transactions on Industry Applications* (2025).

[11] Patra, Prakash Chandra, Pratap Kumar Panigrahi, Anshuman Satpathy, and Niranjan Nayak. "Assessing stability in renewable microgrid using a novel-optimized controller for PV-battery based micro grid with OPAL-RT based real-time validation." *Results in Engineering* 26 (2025): 104290.